

# Investigation of the temperature and precursors concentration dependence of the formation of ZnSe quantum dots

B.A. Duisenbay, T.T. Alibay, A.S. Akhmetova,  
K.B. Zhangylyssov, R.K. Daurenbekova, A.Zh. Kainarbay,  
T.N. Nurakhmetov, D.H. Daurenbekov\*

L.N. Gumilyov Eurasian National University, Astana, Kazakhstan

E-mail: duke.ddx@yandex.ru

DOI: 10.32523/ejpfm.2022060309

Received: 18.08.2022 - after revision

Various variations of the synthesis of ZnSe quantum dots are investigated. The influence of temperature, the concentration of precursors and the time of synthesis of quantum dots was taken into account. Aliquot absorption spectra is measured for various time intervals and the dynamics of the growth of ZnSe quantum dots is estimated. Luminescence and absorption spectra were obtained for purified quantum dots. Based on the experimental data, the nucleation time of quantum dots, optimal methods of synthesis and growth control is determined. HRTEM images showed the average size of ZnSe quantum dot, the calculated band gap is 2.84 eV.

**Keywords:** ZnSe quantum dots; semiconductor; luminescence; absorption; synthesis.

## Introduction

To date, metallic chalcogenide quantum dots (QDs) are attracting increasing interest from scientists, because of their special optical properties. They are mainly used in such areas as: light-emitting diodes (LED), nanolasers, fluorescent probes for biomarkation [1–3]. A potential problem of QDs based on Cd, Pb and Hg is their toxicity. Other objects have been found as an alternative to

them [4]. Quantum dots have high fluorescence yield, high stability and good luminescence, so in recent years they have been widely used in environmental monitoring, food safety testing and biomedicine [5]. One of such objects is zinc selenide (ZnSe) with a large band gap ( $\sim 2.7$  eV), a high coefficient of nonlinear optics, low optical absorption in the visible region, etc. The ZnSe has significant resistance to thermal shock, which makes it the preferred material for optical devices in high-power CO<sub>2</sub> laser systems [6].

In recent years, many studies searching emitters suitable for QD LEDs with blue radiation. Zinc selenide (ZnSe) is the most attractive, as it has a wide direct band gap as well as low toxicity to other materials [7].

The properties of nanoscale semiconductors strongly depend on the crystal structure and size, surface morphology and stoichiometric ratio. Nanoscale characteristics form the properties of the macroscale. ZnSe is a II-VI and n-type semiconductor with a direct band gap energy of 2.7 eV at room temperature [8–9].

For many years, several methods have been adopted for the synthesis of ZnSe nanostructures with different morphologies, such as nanotubes, nanowires, nanoparticles, nanospheres. Different variation is used for the synthesis of ZnSe nanostructures with controlled size, morphology and shape: chemical vapor deposition, molecular beam epitaxy and wet chemical methods [10]. Of these, wet chemical methods are considered a simple, economical, fast, efficient way to synthesize ZnSe nanostructures, since chemical methods do not require complex equipment and are easy to handle [11]. Also, in order to obtain high-quality nanocrystals, synthesis must be carried out at high temperatures using trioctylphosphine and selenium dispersed in 1-octadecene [12]. It was found that a high concentration of surfactant plays a key role in the development of morphology [13].

The emission spectrum depends on the size of the QD and on the potential energy of the charge carriers. This discovery led scientists to the conclusion that the electrical characteristics of a QD depend on its shape and size. This is the peculiarity of QD, due to the fact that its size can be adjusted, it is possible to develop fluorophores of various colors, while not changing the material [14].

To regulate these properties, various experiments are performed with different ligands. The article [15] compares two ligands: OA and ODP. Synthesis was carried out using the "Inverse injection method". It was found that, with an increase in the amount of oleic acid, the size of the QDs increases. The effect of the synthesis temperature on the QDs size was also shown: high temperature leads to the formation of large nanocrystals; the absorption peak shifts to the red region.

ZnSe QDs can be used as matrices for doping, for modification of physico-chemical properties. ZnSe-Al QDs can be promising materials for the development of spectrometric and counting alpha and alpha-beta detectors with high sensitivity and registration efficiency [16] Copper-doped In/ZnSe QDs are used as environmentally friendly fluorescent solar concentrators with high performance [17]. Doping with manganese (ZnSe-Mn) makes it possible to increase the photoluminescence lifetime in transition  ${}^4T_1 \rightarrow {}^6A_1$  in the range of 500–700 nm

[18]. ZnSeZnS core/shell increases chemical stability, enhances optoelectronic and photoluminescent properties. They can be used as probes for detecting  $\text{Cu}^{2+}$  by quenching luminescence [19–21]. In the works, there is no characteristic for narrow luminescence QDs, there is a significant broadening of emission, which may be associated with defects and surface conditions. This phenomenon is insufficiently studied.

In our work, we studied step by step various methods for synthesizing ZnSe QDs with different temperature ranges and precursor concentrations. Experimental data on luminescence and absorption of ZnSe QDs have been obtained. The optimal methods for the synthesis of ZnSe quantum dots are determined.

## Materials and methods

Materials: Zinc Stearate technical grade  $[\text{CH}_3(\text{CH}_2)_{16}\text{COO}]_2\text{Zn}$ , selenium powder (Se,  $\geq 99.9\%$ ), TOP ( $[\text{CH}_3(\text{CH}_2)_7]_3\text{P}$ ,  $\geq 97\%$ ), ODE technical grade ( $\text{CH}_3(\text{CH}_2)_{15}\text{CH}=\text{CH}_2$ ,  $\geq 90\%$ )

Synthesis of QDs was carried out in a 3-necked flask, into which Zinc Stearate 500  $\mu\text{mol}$  (0.3161 g) and ODE (1-octadecene) 12 ml were placed. At this time, Se 500  $\mu\text{mol}$  (0.03948 g) was placed in a specially prepared vial, ODE (1-octadecene) 4 ml and TOP (trioctylphosphine) 1 mmol (0.446 ml) were added there. At  $250^\circ$  a selenium precursor is injected. After injection the timing of synthesis and aliquoting began. The different temperatures synthesis from  $250^\circ$  to  $270^\circ$  and different concentrations of precursors are taken. To observe the intermediate steps of synthesis and nucleation, aliquots were taken during QD growth. To stop further growth of QDs, the synthesis is stopped by abrupt cooling of the solution [14].

Table 1.  
Synthesis parameters.

Sample No.	$\nu(\text{Se})$ , $\mu\text{mol}$	$\nu(\text{TOP})$ , mmol	Time, min	Temperature, $^\circ\text{C}$	Number of aliquots	ODE	
						ZnStearate	Se
1	500	2.42	109	260	6	3	2
2	500	0.22	130	270	4	3	2
3	500	0.22	130	250	4	3	2
4	500	0.22	130	270	-	3	2
5	500	1	166	250	4	12	4
6	500	1	120	250	2	12	4

Absorption spectra were collected with Jasco V-770 spectrometer, photoluminescence spectroscopy was carried out at Solar CM 2203 instrument. HR Transmission electron microscopy studies were performed using Libra 200 (Carl Zeiss, Germany) chromatic aberration-corrected and Tecnai Osiris (FEI, USA) Cs-corrected electron microscopes.

## Results and discussion

Absorption spectrum of ZnSe QD aliquots showing growth kinetics and absorption peak formation, Figure 1. Figure 1a shows that QD nucleation occurs at 45 minutes, a characteristic peak is observed at a wavelength of 402 nm (aliquot no. 2). Aliquots were taken every 15 minutes. With an increase in the synthesis time, the characteristic peak shifts to the long-wavelength region, therefore, the QD grows.

To isolate the resulting QDs from the reaction mixture, staged purification was carried out. To do this, acetone was added to the reaction mass in a ratio of 1:1. The solution was centrifuged at 10,000 rpm for 10 minutes. Purified QDs were dissolved in heptane for further analysis.

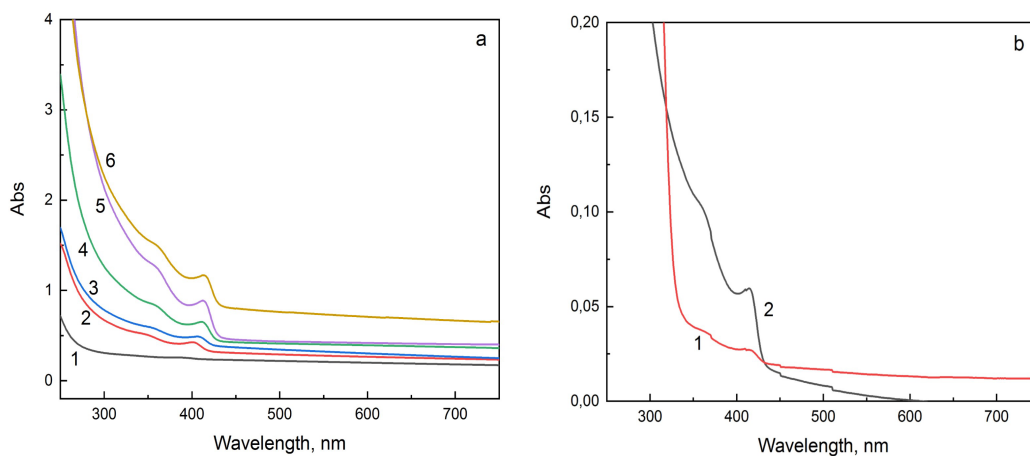


Figure 1. Absorption spectrum of samples, (a) absorption spectrum of aliquots of sample 1, (b) spectrum of purified sample 1.

After QD purification, the peak of the absorption spectrum remained at the same place (416 nm). Therefore, QDs were successfully purified from the total reaction mass. Figure 1b shows curve 1 – the absorption spectrum of the rest of the reaction mass, curve 2 – purified QDs. It can be seen that the purified QDs have a clear absorption peak. However, in band 1, there is a remnant of quantum dots that could not be purified.

Table 2.

Position of absorption peaks of samples 1–6.

Sample	Peak position, nm		
	abs	PL	Begging nucleation
1	416	425	402
2	423	435	418
3	414	426	406
4	419	435	416
5	428	442	412
6	433	428	432

For purified samples, photoluminescence spectra were also obtained. Table 2 shows the position of the peaks of the absorption, PL and QD nucleation spectra.

As can be seen from Table 2, the scatter of values is strongly related to the TOP concentration from Table 1.

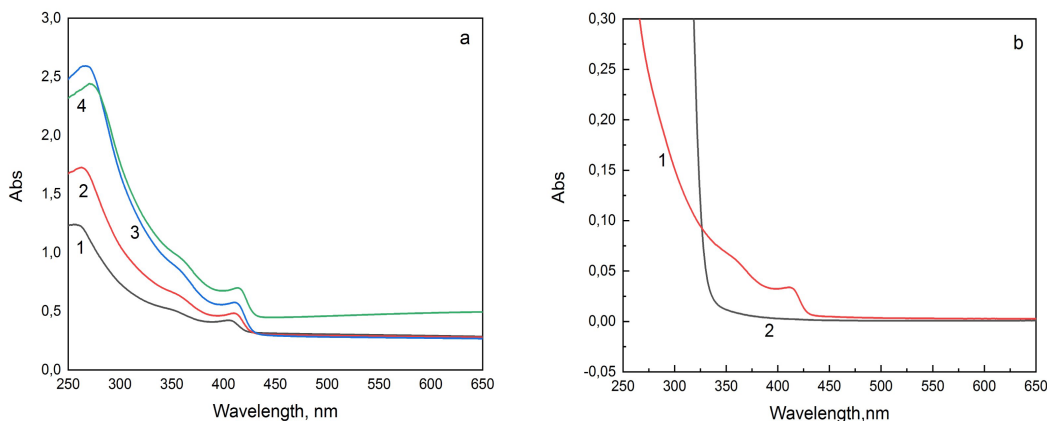


Figure 2. TAbsorption spectrum of samples, (a) absorption spectrum of aliquots sample 3, (b) absorption spectrum of re-purified sample 3.

Figure 2 shows the growth kinetics of QDs, but compared to other (Figure 1a) samples, these peaks are wider. Figure 2a also shows a shift to the long wavelength region, the peak is observed in the region of 417 nm. When this sample was purified, all QDs precipitated, this can be seen in Figure 2b, curve 1 – QD, curve 2 – the rest of the reaction mass. When measuring the absorption spectrum, there were no QDs left in the reaction mass, so the peak in the region of 417 nm is not observed. For better precipitation, it is necessary to repeat the centrifugation procedure.zx

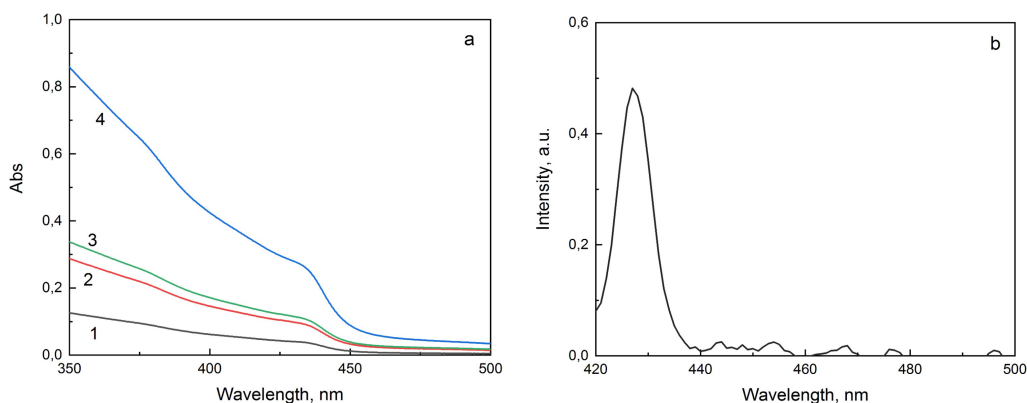


Figure 3. Absorption and luminescence spectrum of samples, (a) absorption spectrum of sample 6, (b) Luminescence spectrum of sample 6.

During the synthesis, it was found that increasing the amount of TOP in solution improves the luminescence spectrum. The spectrum becomes more stable, with a clear narrow peak (Figure 3b). But an increase in the TOP concentration leads to a broadening of the peak of the QD absorption spectrum, as well as to a shift of the peak to a longer wavelength region (Figure 3a). At a given concentration of precursors (sample 6, the TOP concentration is increased), there is no defective band, which indicates the best morphology of the ZnSe QDs samples. Usually, the appearance of a long-wavelength shoulder is associated with defects that are related to selenium vacancies. But in this case, the absence

of a defective band indicates that an excess of TOP promotes an increase in the size of QDs and healing of surface defects.

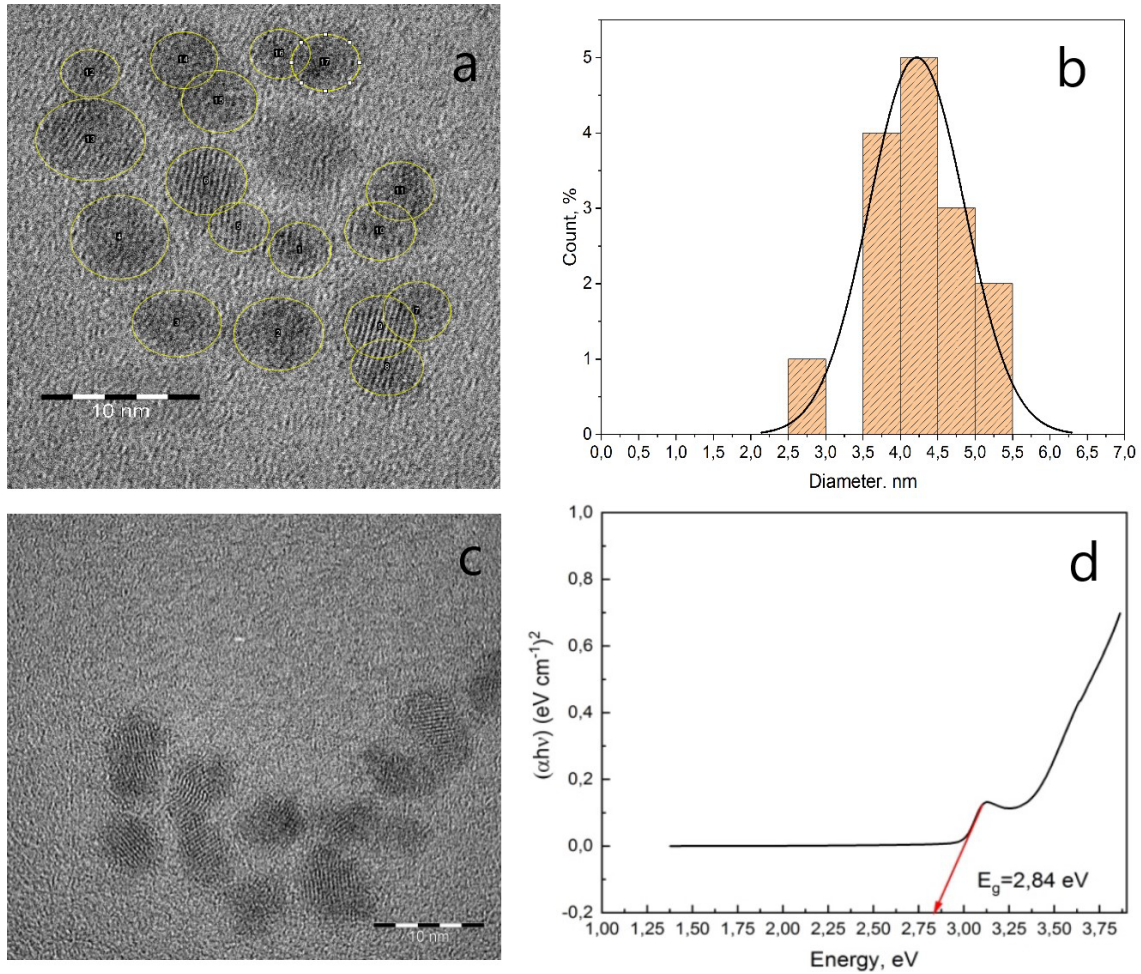


Figure 4. (a) TEM of a ZnSe sample, (b) particle distribution diagram, (c) TEM of a ZnSe sample, (d) calculation of  $E_g$  for a ZnSe sample.

From the TEM patterns, the average particle size of QDs was determined (Figure 4a). It is shown that the resulting ZnSe QDs have a narrow size distribution within 3–5 nm (Figure 4b). Most of them fall on sizes of 3.5–4.5 nm. The band gap of ZnSe QDs was calculated to be 2.84 eV (Figure 4c).

## Conclusion

The main factors that affect the growth of QDs are the temperature and time of synthesis, as well as the amount of precursors. The synthesis temperature affects the growth of QDs, the final size of QDs depends on the synthesis time, the ratio of precursors affects the dispersion and surface stabilization. In particular, an increase in the amount of TOP leads to a broadening of the absorption peak, and also promotes the healing of surface defects. The nucleation of QDs occurs in the time interval of 45–60 minutes in all experiments. The absorption peak, depending on the time and temperature of synthesis, shifts to longer wavelengths, 416 nm at 260° C, 423 nm at 270° C.

## Acknowledgments

This research is funded by the Science Committee of the Ministry of Education and Science of the Republic of Kazakhstan (Grant No. AP08856436).

## References

- [1] P.G. Joshi et al., *Inorganic Chemistry Communications* **135** (2022) 109070. [[CrossRef](#)]
- [2] M.M. Kubenova et al., *Nanomaterials* **11**(9) (2021) 2238. [[CrossRef](#)]
- [3] K.A. Kuterbekov et al., *Ionics* **28** (2022) 4311–4319. [[CrossRef](#)]
- [4] S. Lin et al., *Nano Research* **13** (2020) 824–831. [[CrossRef](#)]
- [5] J. Zhou et al., *Sensors and Actuators: B. Chemical* **305** (2020) 127462. [[CrossRef](#)]
- [6] J. Ke et al., *Superlattices and Microstructures* **156** (2021) 106965. [[CrossRef](#)]
- [7] H.I. Elsaedy et al., *Optics & Laser Technology* **141** (2021) 107139. [[CrossRef](#)]
- [8] I.J. Gonzalez-Panzo et al., *Journal of Crystal Growth* **577** (2022) 126407. [[CrossRef](#)]
- [9] V.S. Patil et al., *Materials Today: Proceedings* **60**(2) (2022) 1099–1102. [[CrossRef](#)]
- [10] T. Gupta et al., *Surfaces and Interfaces* **25** (2021) 101196. [[CrossRef](#)]
- [11] V. Sharma, M.S. Mehata, *Materials Research Bulletin* **134** (2021) 111121. [[CrossRef](#)]
- [12] J.D. Patel, F. Mighri, A. Aji, *Materials Letters* **131** (2014) 366–369. [[CrossRef](#)]
- [13] B. Hou et al., *CrystEngComm* **11** (2009) 1789–1792. [[CrossRef](#)]
- [14] J.Y. Yoo et al., *Journal of Luminescence* **240** (2021) 118415. [[CrossRef](#)]
- [15] H. Shen et al., *Dalton Transactions* **39** (2010) 11432–11438. [[CrossRef](#)]
- [16] G.O. Eren et al., *STAR protocols* **2**(3) (2021) 100664. [[CrossRef](#)]
- [17] J.S. Yu et al., *Materials Letters* **253** (2019) 367–371. [[CrossRef](#)]
- [18] T.A. Nepokupnaya et al., *Nuclear Instruments and Methods in Physics Research Section A: Accelerators, Spectrometers, Detectors and Associated Equipment* **1014** (2021) 165704. [[CrossRef](#)]
- [19] S. Ebrahimi et al., *Journal of Luminescence* **244** (2022) 118757. [[CrossRef](#)]
- [20] S.G. Passos et al., *Journal of Luminescence* **228** (2020) 117611. [[CrossRef](#)]
- [21] J.S. Kim et al., *Journal of Alloys and Compounds* **914** (2022) 165372. [[CrossRef](#)]